DISCLAIMER

This document was prepared as an account of work sponsored by the United States Government. While this document is believed to contain correct information, neither the United States Government nor any agency thereof, nor the Regents of the University of California, nor any of their employees, makes any warranty, express or implied, or assumes any legal responsibility for the accuracy, completeness, or usefulness of any information, apparatus, product, or process disclosed, or represents that its use would not infringe privately owned rights. Reference herein to any specific commercial product, process, or service by its trade name, trademark, manufacturer, or otherwise, does not necessarily constitute or imply its endorsement, recommendation, or favoring by the United States Government or any agency thereof, or the Regents of the University of California. The views and opinions of authors expressed herein do not necessarily state or reflect those of the United States Government or any agency thereof or the Regents of the University of California.

UCRL-1691
Unclassified-Physics Distribution

UNCLASSIFIED

UNIVERSITY OF CALIFORNIA

Radiation Laboratory

Contract No. W-7405-eng-48

FAST MESON INTERACTIONS IN NUCLEAR EMULSIONS

Part I: On π^- Mesons

Hugh Bradner and Bayard Rankin

February 25, 1952

Berkeley, California

FAST MESON INTERACTIONS IN NUCLEAR EMULSIONS

Part I: On π^- Mesons

Hugh Bradner and Bayard Rankin

Radiation Laboratory, Department of Physics
University of California, Berkeley, California

February 25, 1952

ABSTRACT

π^- mesons produced in the Berkeley cyclotron are collimated and monochromatized to 35 ± 2 Mev by a toothed channel in the magnetic field of the cyclotron. Tracks of these mesons obtained in Ilford G5 emulsions are followed and studied for scatter, nuclear stars and disappearances in flight. The energy distribution of the accepted mesons is critically examined and a low energy cut-off for the initial energy is established. 65 percent of the meson track is above 30 Mev in the region of observation, while the remaining 35 percent may drop to 20 Mev. The selection of the high energy particles and their identification by small angle scatter and grain density is discussed. Proton contamination is eliminated largely by small angle scatter. Electrons are ruled out be grain count.

In 902 cm of track there are 5 disappearances and 26 scatters greater than 30°; 4 of the scatters are detectably inelastic, with energy transfer greater than 18 Mev. The combined cross section for stars, disappearances, and inelastic scatters is equal to the cross section for elastic scatters. The measured value for total nuclear interaction is statistically compatible with the combined nuclear area for the responsible elements, oxygen, carbon, bromine, and silver.

FAST MESON INTERACTIONS IN NUCLEAR EMULSIONS

Part I: On π^- Mesons

Hugh Bradner and Bayard Rankin

Radiation Laboratory, Department of Physics
University of California, Berkeley, California

February 25, 1952

Introduction

This paper describes an experiment begun in February, 1950, after discussion with G. Piccioni. At that time cosmic ray evidence(1) implied a cross section for scattering of π^- mesons smaller than nuclear area. Absorptions were the only observed interactions between the high energy(2) mesons and matter. More extensive experiments than ours have subsequently been made on artificially produced mesons by G. Bernardini, et al.(3-6) and others(7-14). Bernardini used a nuclear plate technique similar to that reported here, while the other experimenters have used pure materials as a scatterer. The energy dependence of the interactions in emulsions and pure elements as observed by them and by us is so unexpected that we have decided to report our work in detail.

The present paper should be compared with its companion on π^+ mesons(15).

Experimental Arrangement

π^- mesons produced in the Berkeley cyclotron were collimated and monochromatized to 35.5 $\pm$ 2 Mev by a toothed channel in the magnetic field of the cyclotron. The mesons entered a stack of Ilford G5 plates in a direction parallel to the emulsion surface, and came to rest near the rear edge of the 1 inch wide plates. Individual mesons were selected visually by observing grain count and small angle scatter for approximately 1000μ of

track. These meson tracks were studied for scatter, nuclear stars, and disappearances in flight.

The target and channel used for obtaining the mesons is shown in Fig. 1. π^- mesons leaving the 1/4 x 1/4 inch carbon target with correct energy and direction were brought to rest in the "data" plates. The upper limit of meson energy admitted by the channel is 36.2 Mev and the lower limit is approximately 34.4 Mev. Exception must be made for mesons which scatter from the walls of the channel or leave an unknown target. Teeth of thickness greater than the meson range were provided to minimize the number of scattered mesons.

The channel was 6 inches high. Plates were shielded from stray mesons and nucleons by stacks of 2 x 4 x 8 inch lead bricks, giving a minimum of 6 inches of lead in all horizontal directions except through the channel. The "data" plates were clamped between 1 inch wide blocks of 24 ST aluminum. A second set of plates were clamped similarly and placed in an offset position behind 1 inch of 24 ST aluminum to record μ mesons and other "background" tracks which would have greater than 25.4 mm of range in 24 ST.

Runs in the cyclotron were 15 and 20 seconds. The plates, which were 200μ, 400μ, and 600μ Ilford G5 emulsion, were developed by 100 minute prewash in 35° water, followed by immersion for 5 hours in 3:1 D19 at 35° F. The procedure was suggested by L. Winand. Short-stop was 60 minutes in 1-1/2 percent acetic acid at 68° F. Plates were fixed by agitation for 64 hours in Kodak acid fixer at 72° F. They were then washed for 26 hours and soaked in 25 percent "flexogloss" for 4 hours. After drying, they were lacquered to prevent peeling.

Selection of Mesons

Mesons of 30 to 50 Mev can be distinguished from protons by visual

observation of "wander" or by measurement of small angle scattering vs. grain density. The scan was begun at least 500μ from the edge of the plate to avoid emulsion distortion. For the first 10 percent of the experiment, grain count and small angle scatter measurements were made on all tracks which looked like fast mesons. The measurements extended over 10 segments of 110μ or 158μ. Only tracks which entered the emulsion within 3° of the normal to the plate edge were considered. It became clear that visual check was sufficient to identify a meson in nearly all cases. Accordingly only spot checks were made by grain count and scatter on approximately 1/10 of the remaining 90 percent of the mesons. This is particularly safe since the proton background was only 3 percent.

Accepted tracks were followed to 12 mm from the plate edge or less if the meson left the emulsion in a shorter distance. The track length was computed by using the coordinates of the microscope stage[16] which were read to 10μ accuracy. Segments were considered straight as long as there was no scatter greater than 2°. In the first half of the experiment all scatters which were greater than 2° in the horizontal plane were measured in horizontal projection; during the whole experiment all scatters which were greater than 30° in total angle were measured in both horizontal and vertical projection. Grain counts were made for approximately 1000μ before all scatters greater than 30°, and similar counts were made after each scatter whenever possible. The shrinkage factors ranged from 1.3 to 2.3 and were used in computing vertical components for scatter and grain count. The shrinkage was determined by measuring the unprocessed thickness of test emulsions from the same box as the data plates. We attribute the wide range in shrinkage factor to the flexogloss treatment of the plates.

Locations of all π^- stars in one data plate and one background plate

were recorded in order to establish the spread of energy of incident mesons. Figure 2 is a histogram of frequency vs. energy for these π^- stars. Figure 3, which must be taken in conjunction with it, is a histogram of grain densities at 1 mm into a typical plate for 116 mesons chosen at random from the data. The energy scale shows what energy a π meson would have if the measured grain density were the true one. The dotted histogram of Figure 3 is a Poisson distribution centered at 56 and normalized to 101 particles, the number which remain after subtracting off the left hand tail below 50 Mev. From the evidence of the two histograms it is safe to assume that almost no mesons of incident energy less than 30 Mev were included in the data of the experiment. That is, the measured histogram is consistent with the energy distribution of Figure 2 only if the energy distribution of Figure 2 is cut off at 30 Mev.

The energy was calculated on the assumption that the entire range was in glass of 18 percent[17,18] lower stopping power than emulsion. Meson energy was calculated by converting the range-energy relation[18] for protons in C2 emulsions:

$$E_{Mev} = 0.251\ R_{microns}^{0.581}$$

This relation had been determined experimentally for protons of 32 Mev and less. Ranges corresponding to protons of 200 Mev were required. We made a rough check of the correctness of this relation at high proton energies by comparing it with Aron's[19] calculated ranges in aluminum. The ranges in aluminum were uniformly 10 $\pm$ 1 percent higher than in emulsion for protons of 20 to 200 Mev. The stopping power of 24 ST aluminum was taken to be 1 percent less than emulsion based on the assumption that stopping powers for the elements in the 24 ST were additive. No correction was included for those mesons which made a large angle scatter and stopped

short of their normal range. We ignore the fact that the mesons did not travel their full range in glass.

Note that the yield rose abruptly at 35 Mev and dropped to 3 percent of its maximum at 36.5 Mev, which corresponds to the edge of the data plate. The 1 inch thickness of 24 ST stopped mesons of 39 Mev; hence there is a blank between 36.5 and 39 Mev in the histogram. Energies above 39 Mev were monitored by the background plate. Mesons of the small peak with energies around 52 Mev were included in the experiment. It is assumed that they came from an unknown target. Except for this peak the energy spread of accepted mesons was narrower than the histogram because of the 3° limit on entrance angle and the above mentioned fact that the mesons do not travel all their range in glass. The incident energy is taken to be 35.5 ± 2 Mev.

Scattering measurements were made chiefly to distinguish mesons from protons, and consequently a rapid method could be used. The narrow parallel lines of a specially prepared reticle[20] were oriented with a meson track. The end points of a reticle segment were made to intersect grains of the meson track or the path of the meson as delineated by the grains. Holding the eye piece fixed, the stage was used to translate the meson track through a segment length in the direction of the parallel lines. A displacement was read in microns and the reticle reset as before. Of course, grain counts could be made simultaneously. The mean angle scatter per segment length was taken to be:

$$\bar{\theta} = \arctan \frac{\sum_n |d_i|}{L}$$

where d_i are the displacements, L is the segment length, and n the number of measurements.

Figure 4 is a graph of specific ionization vs. mean angle scatter per 100μ. It is adapted from the curves of Y. Goldschmidt-Clermont[21]. Superimposed on the graph are a number of experimental points obtained by

averaging individual grain count and scattering measurements. Grain density was converted to ionization by assuming linearity in the region[22]. We assumed $G = K(I/I_o)$, where G is average grain density, I/I_o is specific ionization and K is a proportionality constant which must be determined for each plate. K was estimated by $\hat{K} = \hat{G}\ I_o/I(\hat{E})$, where $\hat{G}$ is the mode (or most probable value) of a random sample of grain densities at entrance for particles accepted in a particular plate, and $I(\hat{E})/I_o$ is the specific ionization corresponding to the mode of the energy histogram, Figure 2. Scattering measurements were normalized to give the best fit for the meson measurements. The scattering normalization is justified in this case, since the points are meant to display only the separation of mesons from protons which is obtained by the rapid scattering observation. A normalization is expected, because a displacement method measures a different quantity than the tangential method of Goldschmidt-Clermont. The experimental points of lowest ionization fall to the right of the π meson curve, since they are heavily weighted with μ mesons. They are the only points strongly weighted in this way, because almost any μ meson accepted in the experiment will have specific ionization less than 1.5.

The particles contributing to the meson points of the ionization vs. scattering plot were chosen at random from the accepted data. The proton points were obtained by measuring high energy random background tracks whose orientation would exclude mesons. Therefore, a separate analysis of the measurements would demonstrate the efficiency of the routine selection of mesons at sight. For instance, the forty particles selected at random from the data all fell to the right of the dotted line between the proton and the meson curve, while all but one of the forty background particles fell to the left of it. If one of the particles accepted by sight were actually

measured, it would be separated from the proton group with at least 96 percent probability.

With a reliable method at hand for distinguishing mesons from protons, it is possible to estimate the high energy proton flux within the acceptance angle. The measurements on the incoming tracks that were accumulated over the whole experiment give a proton contamination of less than 3 percent.

Protons having grain density comparable with accepted mesons would suffer little change in grain density while traversing the entire 1 inch of plate, and, therefore, it was possible to get a check on the number of fast protons by scanning the background plate. The number was small, so that a scan was made only to confirm qualitative agreement with the 3 percent obtained by scattering selection.

The possibility of a large high energy electron contamination is excluded on the basis of ionization: positrons in the π-μ decay are hardly visible in identical plates exposed to π^+ mesons. The positrons are soon lost when an attempt is made to trace them.

We assume that the interaction of fast μ^- mesons with matter is a negligible effect in the small percentage of cases when we follow μ mesons. Hence, it is sufficient to correct for μ contamination by estimating the relative flux and correcting the total path length. Any μ mesons should come from energetic π mesons which decayed in flight. Assuming an original parallel beam of π mesons with the energy spread

of 32 to 36 Mev, then the energies of the μ mesons should lie between 8 and 55 Mev. The most energetic ones will come to rest at the back edge of the rear plate. A scan of the control plates and the data plates for σ and ρ endings reveals a μ meson contamination of 10 ± 3 percent. Because of the large statistical error in our measurements, we ignore the fact that approximately five percent of the μ's result in stars.[23-27]

Results

The consistent scanning of high energy meson tracks revealed three types of nuclear events. A high energy meson might scatter, terminate in a star, or disappear. However, the scattering process can be elastic or inelastic while the absorption reaction can yield a single charged particle, more than one, or none at all. Consequently, the events might easily be confused at first sight. Care was taken to distinguish an inelastic scatter from a heavy one prong star and an elastic scatter from a light one prong star. Disappearances have an ambiguous interpretation, since a neutron star looks identical to a charge exchange on a proton:

$$\pi^- + p \Rightarrow n + \pi^0$$

The results of a recent experiment by Wilson and Perry[29] now imply that all our disappearances were neutron stars. The separation of meson scatters and one prong stars was accomplished fairly well with grain count and scattering measurements. In one case the track left the emulsion after 400 mi-

measured, it would be separated from the proton group with at least 96 percent probability.

With a reliable method at hand for distinguishing mesons from protons, it is possible to estimate the high energy proton flux within the acceptance angle. The measurements on the incoming tracks that were accumulated over the whole experiment give a proton contamination of less than 3 percent.

Protons having grain density comparable with accepted mesons would suffer little change in grain density while traversing the entire 1 inch of plate, and, therefore, it was possible to get a check on the number of fast protons by scanning the background plate. The number was small, so that a scan was made only to confirm qualitative agreement with the 3 percent obtained by scattering selection.

The possibility of a large high energy electron contamination is excluded on the basis of ionization: positrons in the π-μ decay are hardly visible in identical plates exposed to π^+ mesons. The positrons are soon lost when an attempt is made to trace them.

We assume that the interaction of fast μ^- mesons with matter is a negligible effect in the small percentage of cases when we follow μ mesons. Hence, it is sufficient to correct for μ contamination by estimating the relative flux and correcting the total path length. Any μ mesons should come from energetic π mesons which decayed in flight. Assuming an original parallel beam of π mesons with the energy spread

of 32 to 36 Mev, then the energies of the μ mesons should lie between 8 and 55 Mev. The most energetic ones will come to rest at the back edge of the rear plate. A scan of the control plates and the data plates for σ and ρ endings reveals a μ meson contamination of 10 ± 3 percent. Because of the large statistical error in our measurements, we ignore the fact that approximately five percent of the μ's result in stars.[23-27]

Results

The consistent scanning of high energy meson tracks revealed three types of nuclear events. A high energy meson might scatter, terminate in a star, or disappear. However, the scattering process can be elastic or inelastic while the absorption reaction can yield a single charged particle, more than one, or none at all. Consequently, the events might easily be confused at first sight. Care was taken to distinguish an inelastic scatter from a heavy one prong star and an elastic scatter from a light one prong star. Disappearances have an ambiguous interpretation, since a neutron star looks identical to a charge exchange on a proton:

$$\pi^- + p \Rightarrow n + \pi^0$$

The results of a recent experiment by Wilson and Perry[29] now imply that all our disappearances were neutron stars. The separation of meson scatters and one prong stars was accomplished fairly well with grain count and scattering measurements. In one case the track left the emulsion after 400 mi-

crons and was classified as a probable one prong star. An event was classified as an inelastic scatter, if there was a statistically significant change in grain density at the scatter point and the resulting particle could be identified as a meson. Such a change in grain density is caused by an energy transfer of not less than 18 Mev.

Fig. 5 is a photomicrograph of a typical meson absorption. The event was found by Mrs. Edith Goodwin and photographed by Mr. A. J. Oliver. Two protons or alpha particles leave the capture point.

The visual characteristics of a "true" meson scatter[30] are shared alike by a "true" scatter, a diffraction scatter, a Coulomb scatter and a π-μ decay. However, the magnitude of deflection in the laboratory system for the latter three events is a strong function of energy. Computations show that for a π meson of 30 Mev and above, only the "true" scatter will attain a magnitude greater than 30° with significant probability. Unfortunately, energy loss in the emulsion will carry 35 percent of our mesons to energies between 20 and 30 Mev, leaving the only absolutely safe scattering limit as 90°. Consequently, mean free paths are computed for scattering greater than 90°. When computing a total interaction mean free path, we assume an equal number of scatters above and below 90°.

Figure 6 is a histogram of the angular distribution in horizontal projection. The data is too meager to justify analysis for the presence of diffraction scattering.

The data is analyzed three ways, in order to check the sensitivity of the results to the low energy tail. Only the first 4.5 mm of each meson track is used, then the rest of the track, and finally all of it. After all the mesons have passed 4.5 mm into the emulsion, the sharp 35 Mev rise point of the energy histogram will become 30 Mev. We then have about 65 percent of the meson track above 30 Mev, while the remaining 35 percent may

drop as low as 20 Mev. Because the mean free paths are statistically the same from the three points of view, we conclude that the energy is high enough and the resolution sharp enough to exclude the confusion from the Coulomb interaction, $\pi - \mu$ decay, and diffraction scattering even in the low energy tail. The important measured quantities are gathered together in Table 3.

Tables 1 and 2 give all the measurements taken on the scatters, stars, and disappearances. The plate thickness is given in the left hand column and a modal grain density (or the most probable value of the grain density) corresponding to almost all plates is given at the right. The mode is obtained by taking the peak value over a random sample of tracks at 1 mm into the plate. It serves as an absolute standard for the energies of the events occurring in each particular plate. For instance, the mode of the random sample is considered to be the grain density for a meson of 34.5 Mev, the mode of the energy distribution in Fig. 2, after correcting for a path length of 1 mm in emulsion.

Conclusions

We have computed the geometrical area presented by the elements of an Ilford emulsion according to:

$$\sigma = \pi \sum_i \frac{N\ell_i}{A_i} (r_o A^{1/3})^2$$

where the summation is taken over the elements of the emulsion. The corresponding mean free path serves as a relative measure with which to compare our total interaction estimates. It is interesting that the two quantities are statistically compatible, suggesting nuclear area as a rough interaction cross section for the individual elements involved. Chedester et al.[9] have added confirming information at 85 Mev by making attenuation

measurements on pure materials. They find cross sections close to nuclear area for a number of elements excluding hydrogen. Their experiments and others[13-14] find hydrogen at less than 1/5 nuclear area for 85 Mev π^- mesons. Emulsion work at this laboratory[15] finds an upper bound of 1/3 nuclear area for 40 Mev π^+ mesons in hydrogen, where nuclear area is taken as $A^{2/3}(\hbar/\mu c)^2$. Because hydrogen presents less than 10 percent of the geometrical area in the emulsion, our results refer essentially to the combined effect of the remaining elements, chiefly oxygen, carbon, bromine, and silver.

The most valuable comparison of our results is made with the Columbia emulsion experiments. Bernardini et al.[3-6] have followed 30-110 Mev π^- mesons through emulsions and found at least two interesting things in contrast to our answers: a greater inelastic scattering cross section and a greater proportion of catastropic events to elastic scatters. Moveover, they find a strong decrease in these quantities with energy, their lowest energy interval being 30-50 Mev. Our 30 Mev values further substantiate the striking drop off of catastrophic events with energy. Only 4 scatters out of 26 are detectably inelastic, while the cross section for elastic scatters is equal to the combined cross section for stars, disappearances and inelastic scatters.

Johnson[31] has pointed out the theoretical importance of these measurements but is unable to explain the prevalence of catastrophic events at high energy or their rapid disappearance with decreasing energy.

Acknowledgments

We wish to thank Dr. G. Piccioni for his original suggestions, and Dr. L. W. Alvarez for his helpful discussions. Mr. J. Kent Bowker was of

great assistance in constructing the channel and making the exposures. We wish to thank especially Mrs. Edith Goodwin who did the majority of the scanning. Her careful work was invaluable and insured a successful and reliable experiment. This work was sponsored by the Atomic Energy Commission.

Information Division
3/6/52 bw

REFERENCES

1. cf for instance W. Fretter - Phys. Rev. 76, 511 (1949)
G. Piccioni - Phys. Rev. 77, 6 (1950)
Brown & McKay - Phys. Rev. 77, 342 (1950)
Harding & Perkins - Nature 164, 285 (1949)

2. The energy was not well defined, but in almost all measurements was over 150 Mev.

3. G. Bernardini, E. T. Booth, L. Lederman, and J. Tinlot, Phys. Rev. 80, 924 (1950)

4. G. Bernardini, E. T. Booth, L. Lederman, and J. Tinlot, Phys. Rev. 82, 105 (1951)

5. G. Bernardini, E. T. Booth, and L. Lederman, Phys. Rev. 83, 1075 (1951)

6. G. Bernardini, E. T. Booth, and L. Lederman, Phys. Rev. 83, 1277 (1951)

7. M. Skinner and C. Richman, Phys. Rev. 83, 217(A) (1951)

8. M. Camac, D. R. Corson, D. Littaver, H. M. Shapiro, A. Silverman, R. R. Wilson, W. M. Woodward, Phys. Rev. 82, 745 (1951)

9. C. Chedester, P. Isaacs, A. Sachs, and J. Steinberger, Phys. Rev. 82, 958 (1951)

10. A. M. Shapiro, Phys. Rev. 83, 874(a) (1951)

11. H. Byfield, J. Kessler and L. Lederman, B.A.P.S. 26, No. 6, 22 (1951)

12. P. Isaacs, A. Sachs, and J. Steinberger, same

13. R. P. Shutt, E. C. Fowler, D. H. Miller, A. M. Thorndike, and W. B. Fowler, Phys. Rev. 84, 1247 (1951)

14. E. Fermi, H. L. Anderson, A. Lundy, D. E. Nagle, and G. B. Yodh, Phys. Rev. to be published. Also, H. L. Anderson, E. Fermi, E. A. Long, R. Martin, and D. E. Nagle, Phys. Rev. to be published

15. Bayard Rankin and Hugh Bradner, Part II of this paper, Phys. Rev.

16. The stage was designed and made by Mr. William M. Brower.

17. L. Winand, Private communication

18. Hugh Bradner, Frances M. Smith, Walter H. Barkas, and H. S. Bishop, Phys. Rev. 77, 462 (1950)

19. W. A. Aron, B. G. Huffman, R. C. Williams, UCRL-121 (1949)

20. The reticles were made by D. J. O'Connell

21. Y. Goldschmidt-Clermont, Bulletin du Centre de Physique Nucléaire de L'Université Libre de Bruxelles, No. 14 (1949)

22. J. Kent Bowker, John R. Green, and W. H. Barkas, Phys. Rev. 81, 649(A) (1951)

23. E. P. George and J. Evans, Proc. Phys. Soc. 611 (1951)

24. G. W. McClure, Phys. Rev. 83, 207(A) (1951)

25. G. Cocconi and V. Cocconi Tongiorgi, Phys. Rev. 84, 29 (1951)

26. Satio Hagakawa, Phys. Rev. 84, 37 (1951)

27. D. F. Sherman, Harry H. Heckman, and Walter H. Barkas, BAPS, 26, No. 8, 23 (1951)

28. J. Ashkin, A. Simon, and R. Marshak, Prog. Theor. Phys. V, 634 (1950)

29. Richard Wilson and John P. Perry, Phys. Rev. 84, 163 (1951)

30. S. Fernbach, R. Serber, and T. B. Taylor, Phys. Rev. 75, 1352 (1949)

31. M. H. Johnson, Phys. Rev. 83, 510 (1951)

TABLE 1

LARGE ANGLE SCATTERS

Type of Plate (thickness)	Angle (degrees) Horizontal Projection	Angle (degrees) Total	Distance in Plate (mm)	Grain Density/100μ (1) Before	Grain Density/100μ (1) After	Modal Grain (1) density at 1 mm for accepted track
400	29	30	2.8	38 ± 1.5	36 ± 1.5	--
300	32	32	6.2	20 ± 1.1	23 ± 1.2	40.9 ± 0.9
400	20	32	1.0	37 ± 2.1	42 ± 5.6	36.5 ± 0.6
400	35	35	7.4	37 ± 1.5	--	36.3 ± 0.6
600	30	35	10.6	25 ± 1.3	25 ± 1.9	--
400	29	37	4.0	36 ± 1.5	36 ± 2.7	36.5 ± 0.3
400	0	45	2.1	35 ± 1.5	30 ± 2.7	36.3 ± 0.6
300	44	46	3.3	*39 ± 1.6	68 ± 5.8	40.9 ± 0.9
300	44	46	1.8	41 ± 1.6	43 ± 3.6	40.9 ± 0.9
400	6	46	2.2	35 ± 2.0	29 ± 5.0	--
400	40	48	1.2	33 ± 1.9	38 ± 4.4	--
600	50	50	7.6	*31 ± 1.4	38 ± 1.6	35.4 ± 0.8
400	56	57	1.5	33 ± 1.4	37 ± 2.0	36.3 ± 0.6
400	12	70	0.8	38 ± 2.2	--	36.3 ± 0.6
200	47	76	2.0	†55 ± 2.6	52 ± 6.8	--
400	104	102	8.6	38 ± 1.5	42 ± 3.4	36.3 ± 0.6
400	108	105	9.0	38 ± 2.1	38 ± 3.6	--
400	121	109	0.8	31 ± 2.0	34 ± 2.5	36.3 ± 0.6
200	119	112	5.7	47 ± 2.4	64 ± 11.0	--
200	143	123	1.3	†*64 ± 2.4	99 ± 7.4	--
300	166	141	2.2	37 ± 1.5	--	40.9 ± 0.9
600	151	145	2.9	34 ± 1.8	36 ± 2.8	34.7 ± 0.7
600	158	154	11.1	*39 ± 1.6	56 ± 3.8	--
600	171	155	2.2	37 ± 2.1	34 ± 2.8	--
400	167	158	2.5	35 ± 1.5	35 ± 1.9	36.3 ± 0.6
400	178	160	3.8	35 ± 1.5	35 ± 2.8	36.3 ± 0.6

(1) The errors are standard deviations.

* Inelastic scatter.

† Abnormally low energy.

TABLE 2

STARS

Type of Plate (Thickness)	Number of Prongs	Distance in plate (mm)	Grain Density /100μ (1) Before event	Model grain (1) density at 1 mm for Accepted Track
400	1	5.4	37 ± 1.5	36.5 ± 0.3
400	1	0.7	37 ± 1.7	36.5 ± 0.3
400	1	10.4	†41 ± 1.6	36.5 ± 0.3
400	1	4.2	36 ± 1.5	36.3 ± 0.6
400	1	1.7	36 ± 1.5	36.3 ± 0.6
300	1	1.4	41 ± 1.6	40.9 ± 0.9
300	1	6.1	41 ± 1.6	40.9 ± 0.9
400	2	8.5	--	--
400	2	1.6	37 ± 1.5	36.3 ± 0.6
400	2	1.3	†41 ± 1.6	36.3 ± 0.6
600	2	3.8	32 ± 1.4	35.4 ± 0.8
			STOPS	
400		3.0	35.0 ± 1.5	36.3 ± 0.6
400		3.2	34.5 ± 1.5	36.3 ± 0.6
600		6.2	31.0 ± 2.6	35.4 ± 0.8
600		9.1	†40.3 ± 1.6	35.4 ± 0.8
600		2.3	34.4 ± 1.5	35.4 ± 0.8

(1) The errors are standard deviations.

† Abnormally low energy.

TABLE 3

SUMMARY OF RESULTS

	Using first 4.5 mm of each track	Using all but first 4.5 mm	Using all the track (1)
Total Path Length Scanned (cm) (Corrected for 10 percent μ^- contamination	582	320	902 ± 30
Number of disappearances in flight	3	2	5
Number of Stars	7	4	11
1 Prong			7
2 Prongs			4
Number of Scatters greater than 30°	18	8	26
Number of Scatters greater than 90°	7	4	11
Mean Free Path for Disappearances (cm)	194	160	180 ± 55
Mean Free Path for Stars (cm)	83	80	82 ± 17
Mean Free Path for Scatters greater than 90° (cm)	83	80	82 ± 17
Mean Free Path for Total Nuclear Interaction (cm) (Assuming symmetry about 90°)	24.2	22.9	23.7 ± 3.2
Mean Free Path Corresponding to Nuclear Area (cm) (for emulsion)			23

(1) The errors are probable errors.

Captions to the Figures

Fig. 1 - The target and channel assembled on a cart and ready to be rolled through a port in the cyclotron tank wall. The 1/4 x 1/4 carbon target is mounted on a lead brick in the foreground.

Fig. 2 - Histogram of frequency vs. energy for the incident mesons. Mesons of incident energy less than 30 Mev were largely excluded by grain density observations.

Fig. 3 - Histogram of grain densities at 1 mm into a typical plate for 116 mesons chosen at random from the data. The energy scale shows what energy a π meson would have if the measured grain density were the true one. The dotted histogram is a Poisson distribution.

Fig. 4 - Specific ionization vs. mean angle scatter per 100μ. The heavy lines are the curves of Y. Goldschmidt-Clermont. Experimental points near the meson curve represent a sample of the data and are given with probable errors. The remaining three points are background.

Fig. 5 - Photomicrograph of a typical meson absorption. The event was found by Mrs. Edith Goodwin and photographed by Mr. A. J. Oliver. Two protons or alpha particles leave the capture point.

Fig. 6 - Histogram of the angular distribution of scatters in horizontal projection.

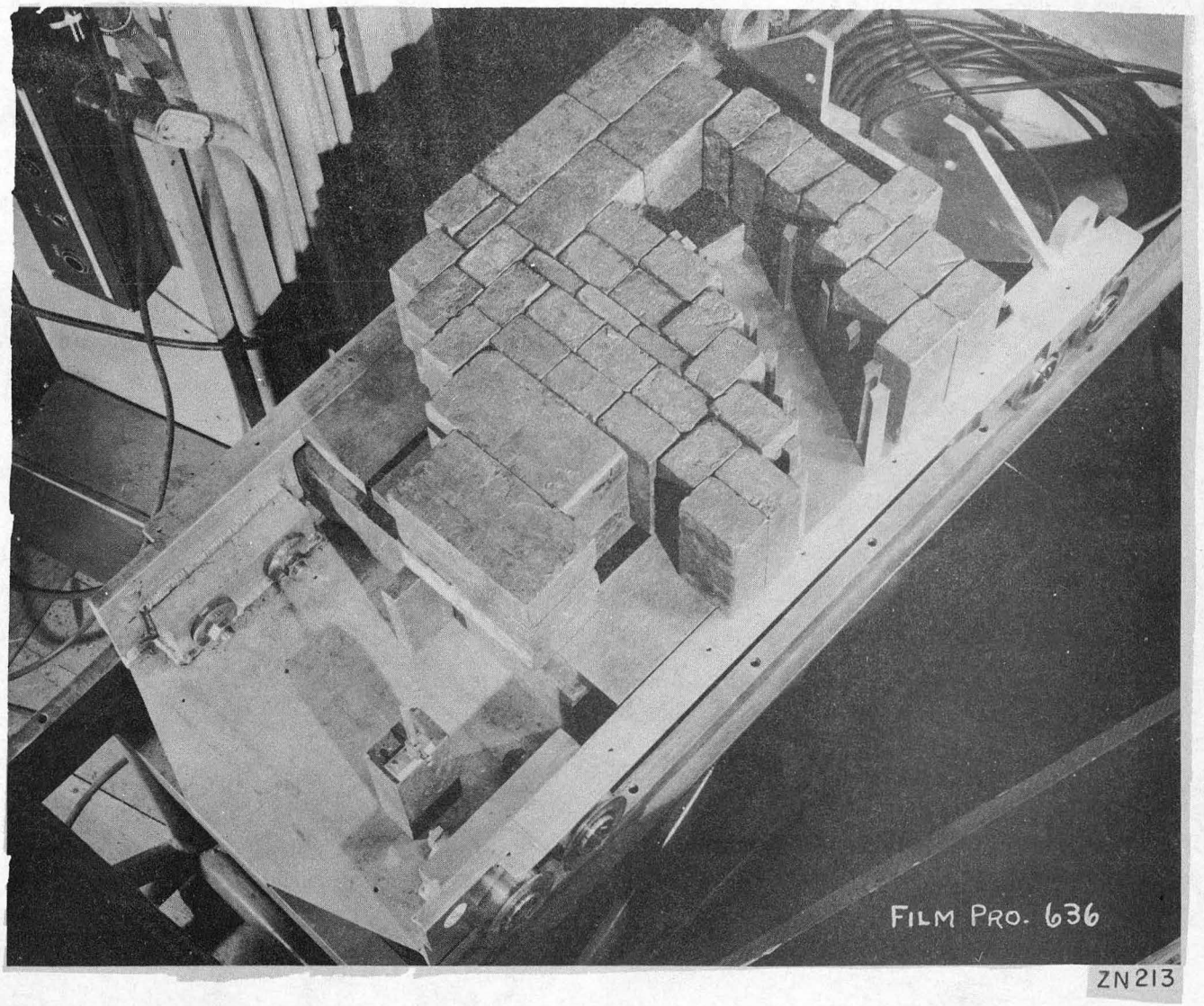

ZN213

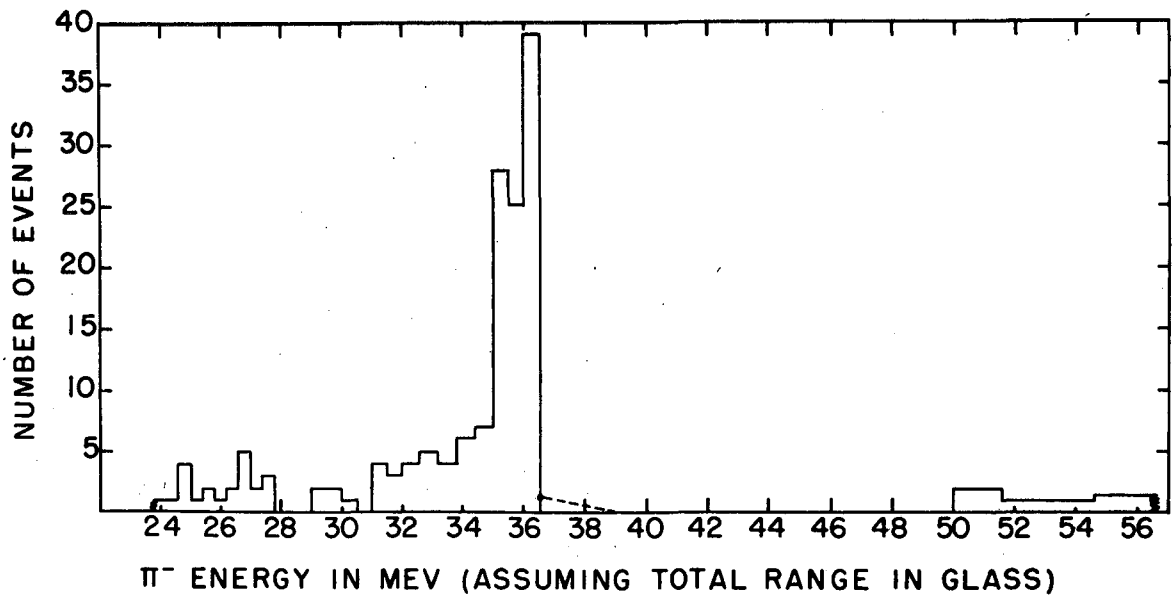
NUMBER OF EVENTS
40
35
30
25
20
15
10
5
24 26 28 30 32 34 36 38 40 42 44 46 48 50 52 54 56
π⁻ ENERGY IN MEV (ASSUMING TOTAL RANGE IN GLASS)

Fig. 2

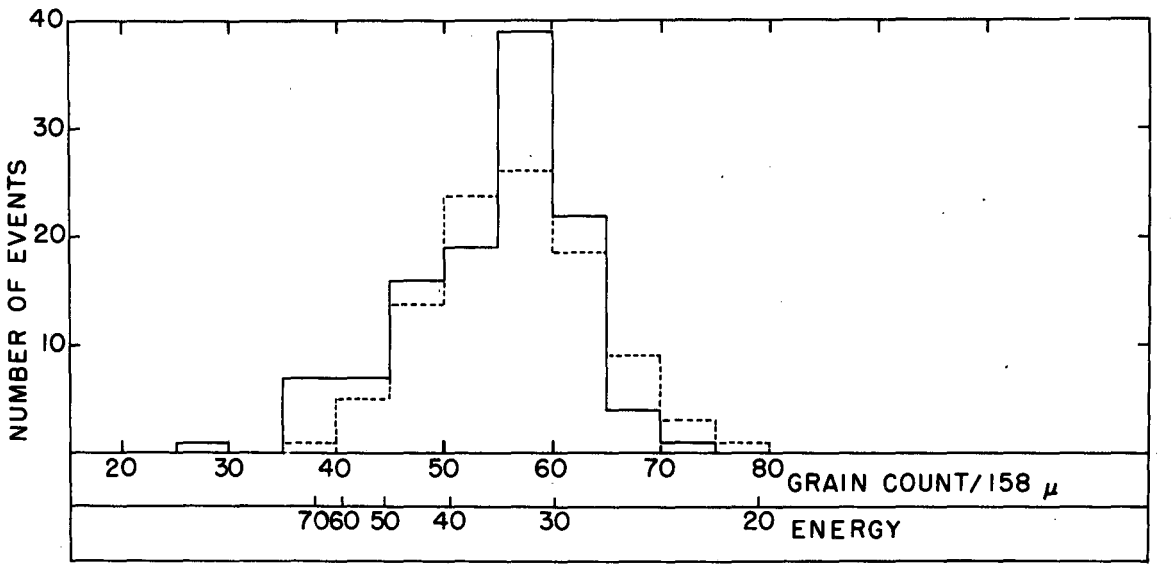
NUMBER OF EVENTS
40
30
20
10
20
30
40
50
60
70
80
GRAIN COUNT/158 μ
70
60
50
40
30
20
ENERGY

Fig. 3

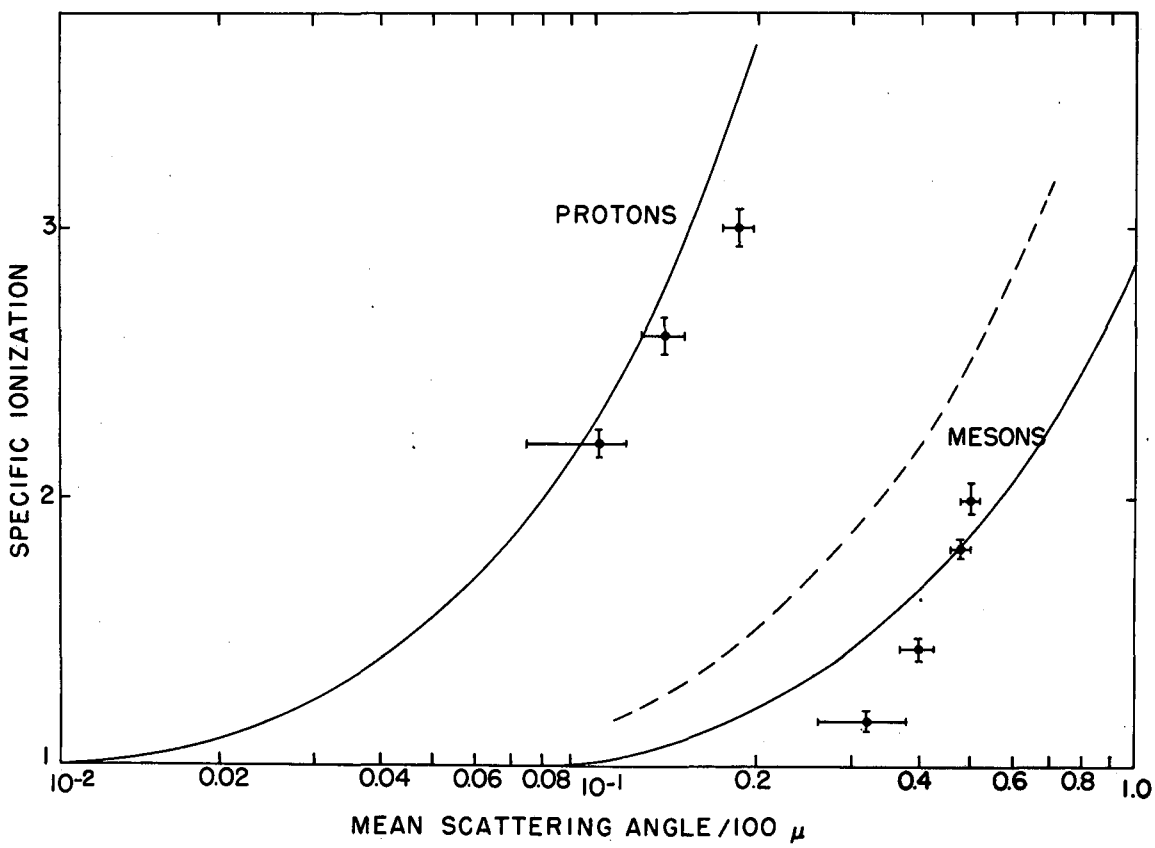
PROTONS
MESONS
SPECIFIC IONIZATION
3
2
1
10-2
0.02
0.04
0.06
0.08
10-1
0.2
0.4
0.6
0.8
1.0
MEAN SCATTERING ANGLE /100 μ

Fig. 1

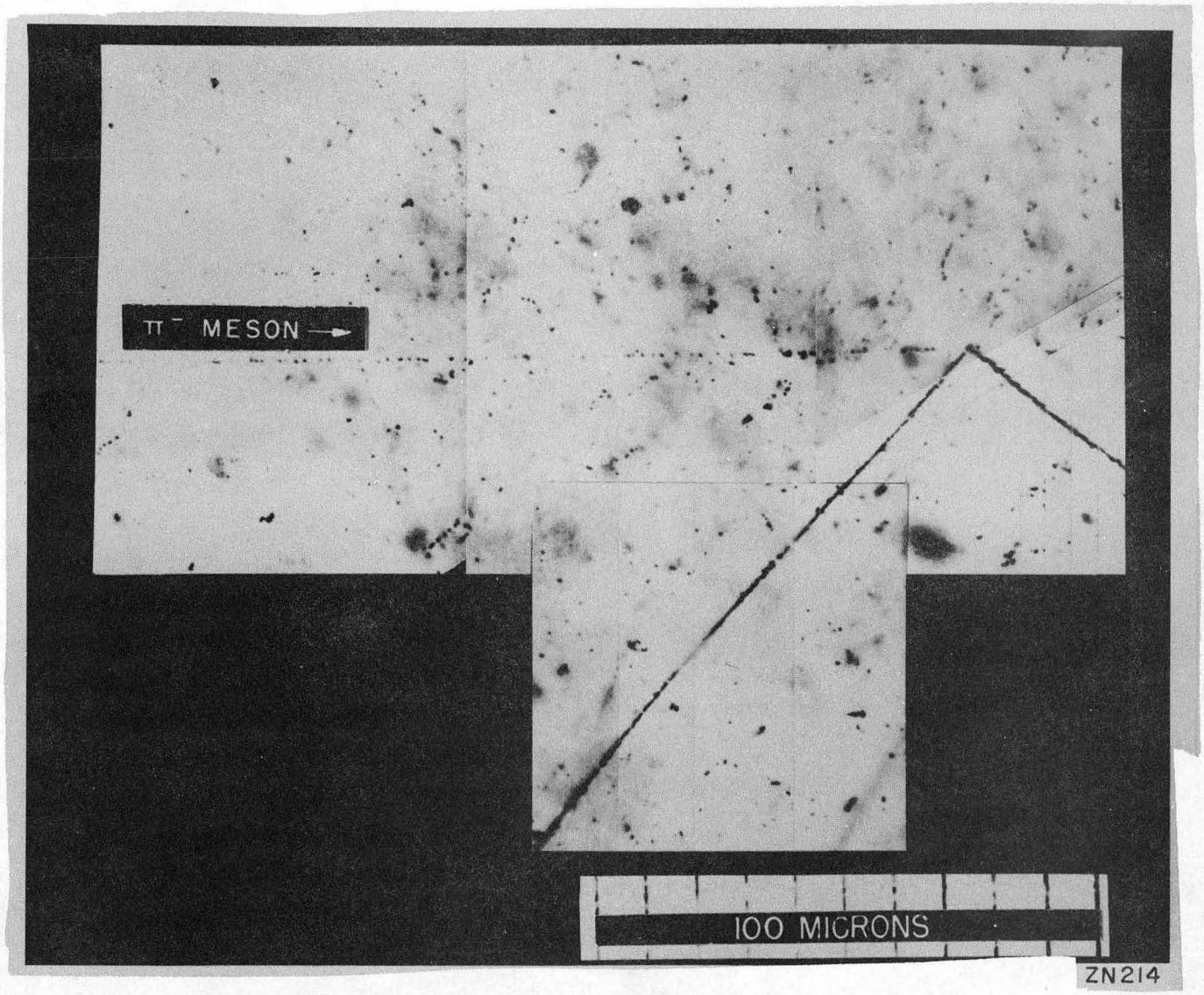

Fig. 5

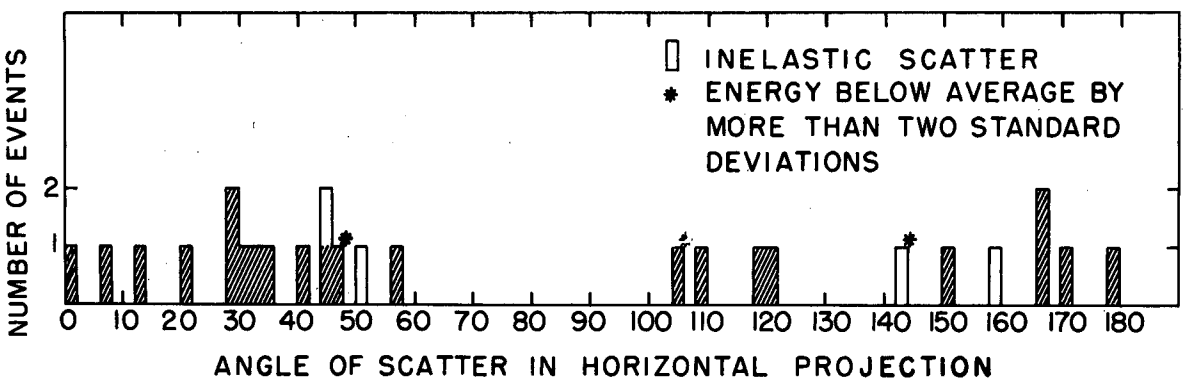
INELASTIC SCATTER
ENERGY BELOW AVERAGE BY MORE THAN TWO STANDARD DEVIATIONS
NUMBER OF EVENTS
2
1
0 10 20 30 40 50 60 70 80 90 100 110 120 130 140 150 160 170 180
ANGLE OF SCATTER IN HORIZONTAL PROJECTION

Fig. 6